Supporting Information

Photothermal therapy for cancer cells by optically tunable Fe_2O_3@Au hexagonal nanodisks

Lin Li[a], Fenglian Qi[a,b], Jiong Guo [a], Jing Fan [a], Wenxiang Zheng [aa], Murtaza Ghulam[a], and Weizhi Wang[a], Zihui Meng[*,a,c], Lili Qiu[*]

[a] *School of Chemistry and Chemical Engineering, Beijing Institute of Technology, Beijing 100081, P. R. China.*
[b] *CAS Key Laboratory of Nanosystem and Hierarchical Fabrication, CAS Center for Excellence in Nanoscience, National Center for Nanoscience and Technology, Beijing 100190, P. R. China.*
[c] *Yangtze Delta Region Academy of Bejing Institute of Technology, Jiaxing 314019, P. R. China.*
E-mail: m_zihui@yahoo.com
E-mail: qiulili@bit.edu.cn

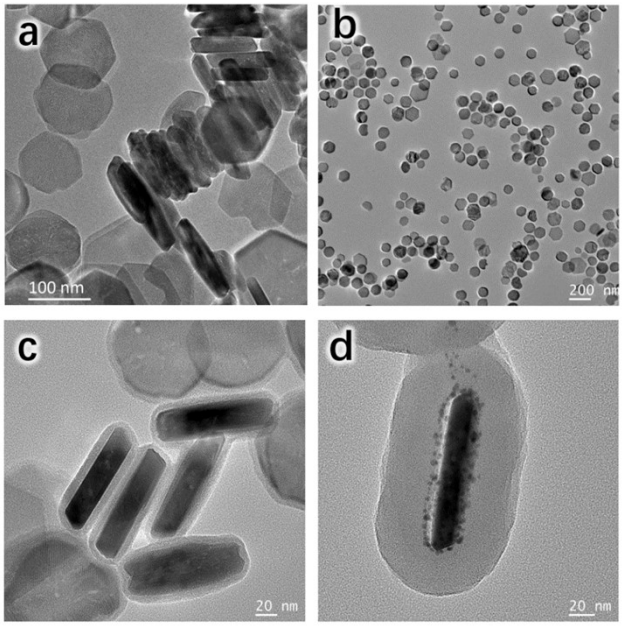

Supplementary Figure 1. TEM images of (a) Fe_2O_3, (b)Fe_2O_3@SiO_2, and the side of (c) Fe_2O_3@SiO_2, (d)Fe_2O_3@void@Au seeds@RF,

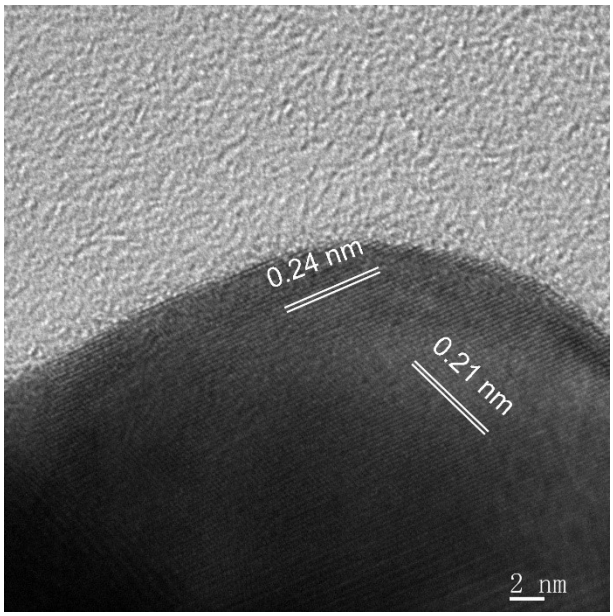

Supplementary Figure 2 HRTEM of 120 nm Fe_2O_3@Au From the HR-TEM image, the lattice spacing is 0.24 nm and 0.21 nm, which correspond to the (111) and (200) crystal planes of Au, respectively.

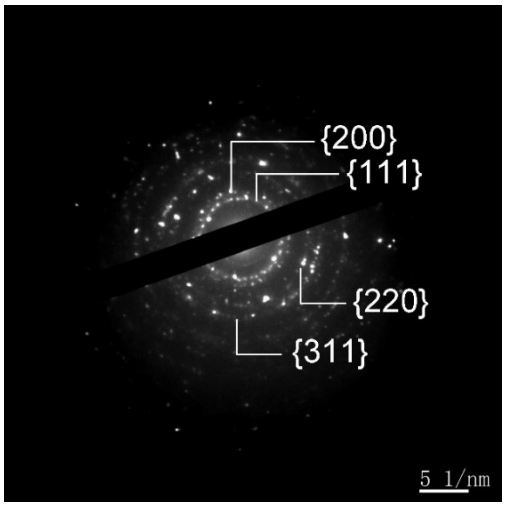

Supplementary Figure 3. SAED pattern of 120 nm Fe_2O_3@Au. The polycrystalline diffraction rings in the SAED pattern confirmed typical crystal planes of (111), (200), (220), (311) of Au.

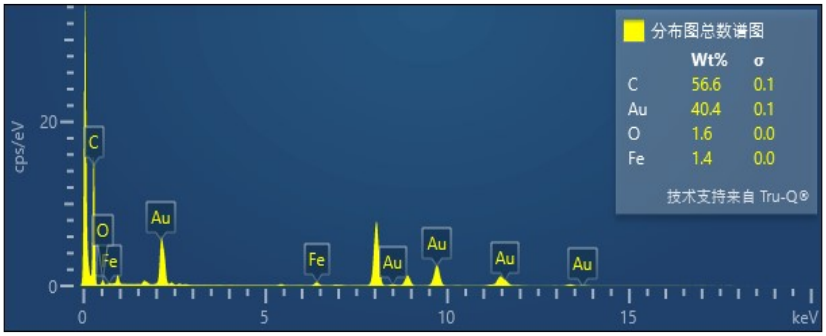

Supplementary Figure 4. Elemental distribution spectrum of 120 nm Fe_2O_3@Au@RF

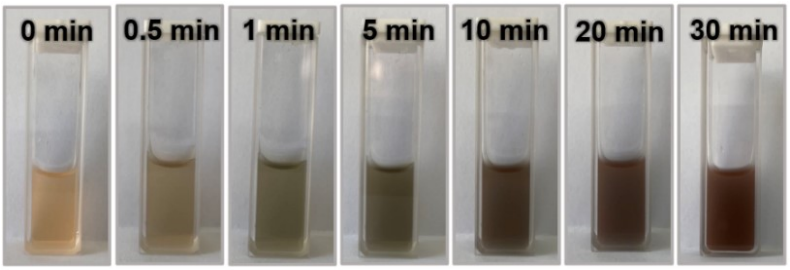

Supplementary Figure 5. The color of reaction solution during the growth of Au nanoshells.

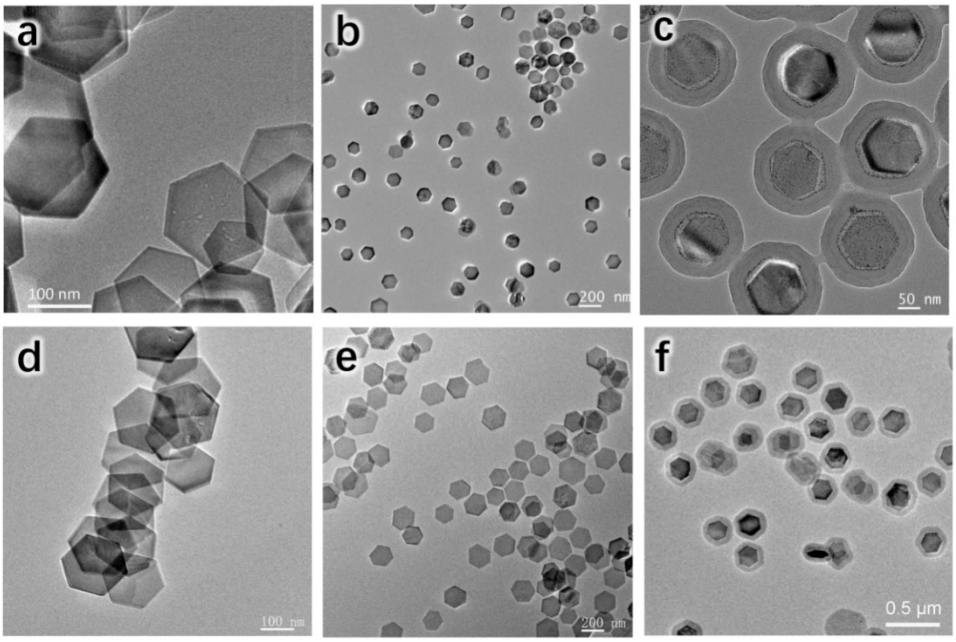

Supplementary Figure 6. TEM images of Fe_2O_3 with the size of (a) 160 nm, (d) 210 nm, Fe_2O_3@SiO_2 with the Fe_2O_3 size of (b) 160 nm and (e) 210 nm, and Fe_2O_3@void@Au seeds@RF with the Fe_2O_3 size of (c) 160 nm and (f) 210 nm.

Table S1. The specific size of the AuNDs

diagonal size of Fe_2O_3(nm)	thickness of Fe_2O_3(nm)	thickness of RF(nm)	thickness of Au NDs(nm)	diagonal size of Au NDs(nm)
120	21	24	56	155
160	19	23	67	190
210	24	34	80	265

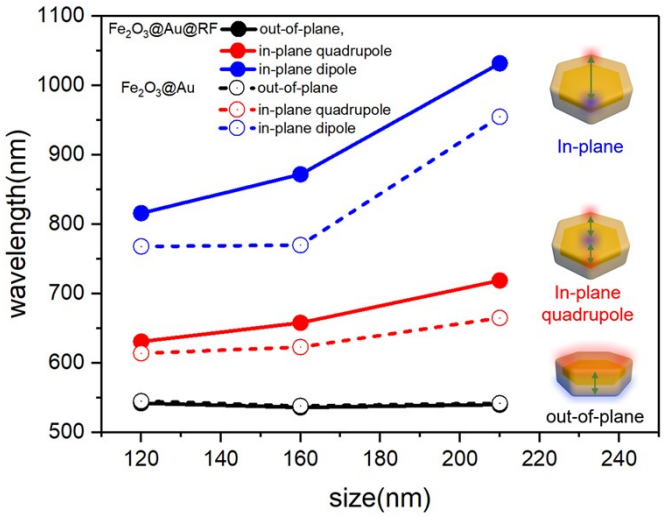

Supplementary Figure 7. The extinction peak positions of different sizes of NDs

Table S2. Summary of the parameters used for the calculation of the heat conversion efficiency. Were applicable, errors on the last digit are given in parentheses

	m	Cp	ΔT	τs	I (W)	QD	η
Fe_2O_3@Au@RF	0.5	4.186	43.5	243	1	0.337816	47%
Water	0.5	4.186	9.8	170	1		

Table S3. The photothermal conversion efficiency of various of materials

Materials	Laser (nm)	Time (min)	Power density ($W \cdot cm^{-2}$)	ΔT (℃)	Concentration ($mg \cdot ml^{-1}$)	η	Ref.
Gold hollow NRs	1064	5	0.2	35	0.15	33%	1
Miniature hollow Gold	1064	10	0.7	17	0.0732	34%	2
miniature Au/Ag NRs	1064	10	0.8	23.2	0.1	28.8%	3
Gold nano-frameworks	1064	6	1	27.5	0.2	32.9%	4
Gold nanostars	1064	5	1	14.3	0.1	36.4%	5
Chitosan-carbon dot	808	5	1.5	57	0.2	25.2%	6
Carbon Dots	808	8	1.4	25	0.02	30.6%	7
Bi@C nanoparticles	1064	10	1	25.6	0.4	43.2%	8
Cu_3BiS_3	1064	6	1	30	0.1	40.7%	9
$Cu_{2-x}S$ nanodots	1064	5	1	30	0.1	30.8%	10
Ni_9S_8 nanoparticles	1064	10	0.7	20	0.1	46%	11
CuS-Au heterostructures	1064	5	1.5	40	0.06	36.5%	12
$FePS_3$ nanosheets	1064	10	2	25	0.024	43.3%	13
Metallic 1T Phase-MoS_2	1064	5	1	43	0.5	43.3%	14
Er: WSe_2	808	10	0.6	42	0.2	35.2%	15
H2a-4T+FBS	808	10	0.15	42.4	0.008	20.6%	16
PDCDT	808	6	0.3	40.2	0.2	44.9%	17
SPN	1064	10	1	28	0.03	46%	18
L1057 NPs	980	8	1	30.3	0.1	38%	19
TMB-F4TCNQ	1064	10	1	22.4	0.1	42.4%	20
Fe_2O_3@Au@RF	808	8	1	43.5	0.1	47%	This work

References

[1] K. Cai, W. Zhang, J. Zhang, H. Li, H. Han, T. Zhai, ACS Appl Mater Interfaces, 10 (2018) 36703-36710.

[2] K. Cai, W. Zhang, M.F. Foda, X. Li, J. Zhang, Y. Zhong, H. Liang, H. Li, H. Han, T. Zhai, Small, 16 (2020) e2002748.

[3] Z. Mei, D. Gao, D. Hu, H. Zhou, T. Ma, L. Huang, X. Liu, R. Zheng, H. Zheng, P. Zhao, J. Zhou, Z. Sheng, Biomaterials, 251 (2020) 120092.

[4] J. Wang, J. Sun, Y. Wang, T. Chou, Q. Zhang, B. Zhang, L. Ren, H. Wang, Adv. Funct. Mater., 30 (2020).

[5] D. Zhu, M. Lyu, Q. Huang, M. Suo, Y. Liu, W. Jiang, Y. Duo, K. Fan, ACS Appl Mater Interfaces, 12 (2020) 36928-36937.

[6] H. Wang, S. Mukherjee, J. Yi, P. Banerjee, Q. Chen, S. Zhou, ACS Appl Mater Interfaces, 9

(2017) 18639-18649.
[7] Y. Li, G. Bai, S. Zeng, J. Hao, ACS Appl Mater Interfaces, 11 (2019) 4737-4744.
[8] W. Zhen, S. An, W. Wang, Y. Liu, X. Jia, C. Wang, M. Zhang, X. Jiang, Nanoscale, 11 (2019) 9906-9911.
[9] A. Li, X. Li, X. Yu, W. Li, R. Zhao, X. An, D. Cui, X. Chen, W. Li, Biomaterials, 112 (2017) 164-175.
[10] R. Hu, Y. Fang, M. Huo, H. Yao, C. Wang, Y. Chen, R. Wu, Biomaterials, 206 (2019) 101-114.
[11] Z. Lei, W. Zhang, B. Li, G. Guan, X. Huang, X. Peng, R. Zou, J. Hu, Nanoscale, 11 (2019) 20161-20170.
[12] Z. Wang, N. Yu, X. Li, W. Yu, S. Han, X. Ren, S. Yin, M. Li, Z. Chen, Chem. Eng. J., 381 (2020) 122613.
[13] Q. Zhang, Q. Guo, Q. Chen, X. Zhao, S.J. Pennycook, H. Chen, Adv. Sci. (Weinheim, Ger.), 7 (2020) 1902576.
[14] Z. Zhou, B. Li, C. Shen, D. Wu, H. Fan, J. Zhao, H. Li, Z. Zeng, Z. Luo, L. Ma, C. Tan, Small, 16 (2020) e2004173.
[15] Y. Huang, Y. Zhao, Y. Liu, R. Ye, L. Chen, G. Bai, S. Xu, Chem. Eng. J., 411 (2021) 128610.
[16] X. Zeng, Y. Xiao, J. Lin, S. Li, H. Zhou, J. Nong, G. Xu, H. Wang, F. Xu, J. Wu, Z. Deng, X. Hong, Adv. Healthcare Mater., 7 (2018) e1800589.
[17] Y. Jiang, J. Li, X. Zhen, C. Xie, K. Pu, Adv. Mater., 30 (2018) e1705980.
[18] T. Sun, J. Han, S. Liu, X. Wang, Z.Y. Wang, Z. Xie, ACS Nano, 13 (2019) 7345-7354.
[19] Y. Yang, X. Fan, L. Li, Y. Yang, A. Nuernisha, D. Xue, C. He, J. Qian, Q. Hu, H. Chen, J. Liu, W. Huang, ACS Nano, 14 (2020) 2509-2521.
[20] C. Ou, W. Na, W. Ge, H. Huang, F. Gao, L. Zhong, Y. Zhao, X. Dong, Angew. Chem., Int. Ed. Engl., 60 (2021) 8157-8163.

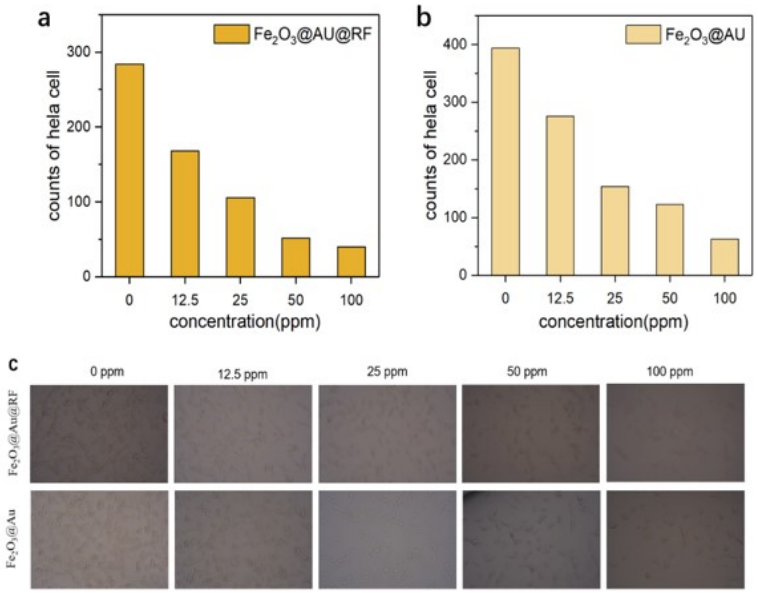

Supplementary Figure 8. Statistics of the number of Hela cells after adding different concentrations of (a) Fe_2O_3@Au@RF and (b) Fe_2O_3@Au nanosheets after laser irradiation for

3 min, and (c) the corresponding optical photos of cells (×10)